

ORNL  
REPRODUCTION COPY

DATE ISSUED

APR 29 1974

ORNL-TM-4541

# EFFECT OF HIGH HELIUM CONTENT ON STAINLESS STEEL SWELLING

F. W. Wiffen

E. E. Bloom



**OAK RIDGE NATIONAL LABORATORY**

OPERATED BY UNION CARBIDE CORPORATION • FOR THE U.S. ATOMIC ENERGY COMMISSION



ORNL-TM-4541

Contract No. W-7405-eng-26

METALS AND CERAMICS DIVISION

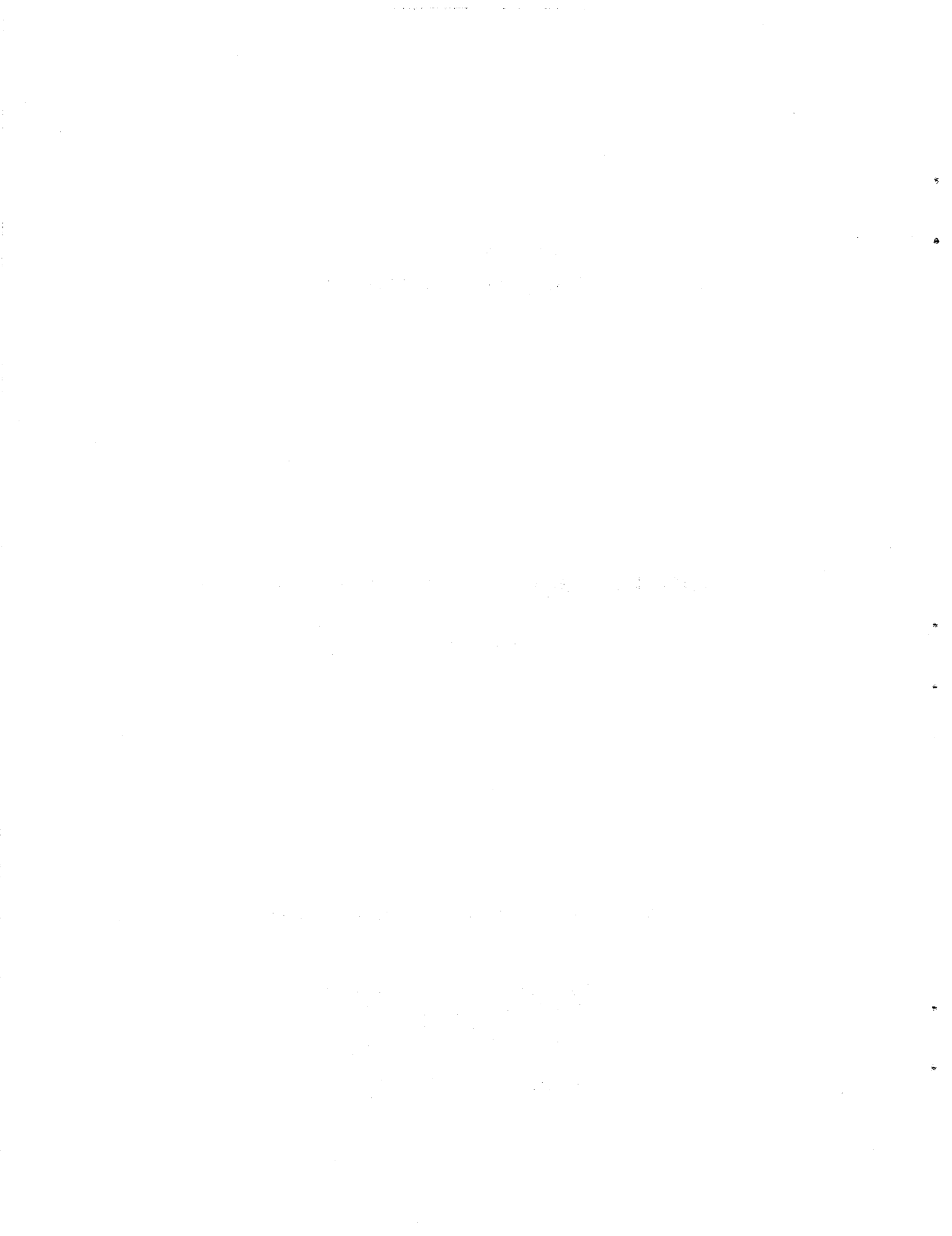
EFFECT OF HIGH HELIUM CONTENT ON STAINLESS STEEL SWELLING

F. W. Wiffen and E. E. Bloom

MAY 1974

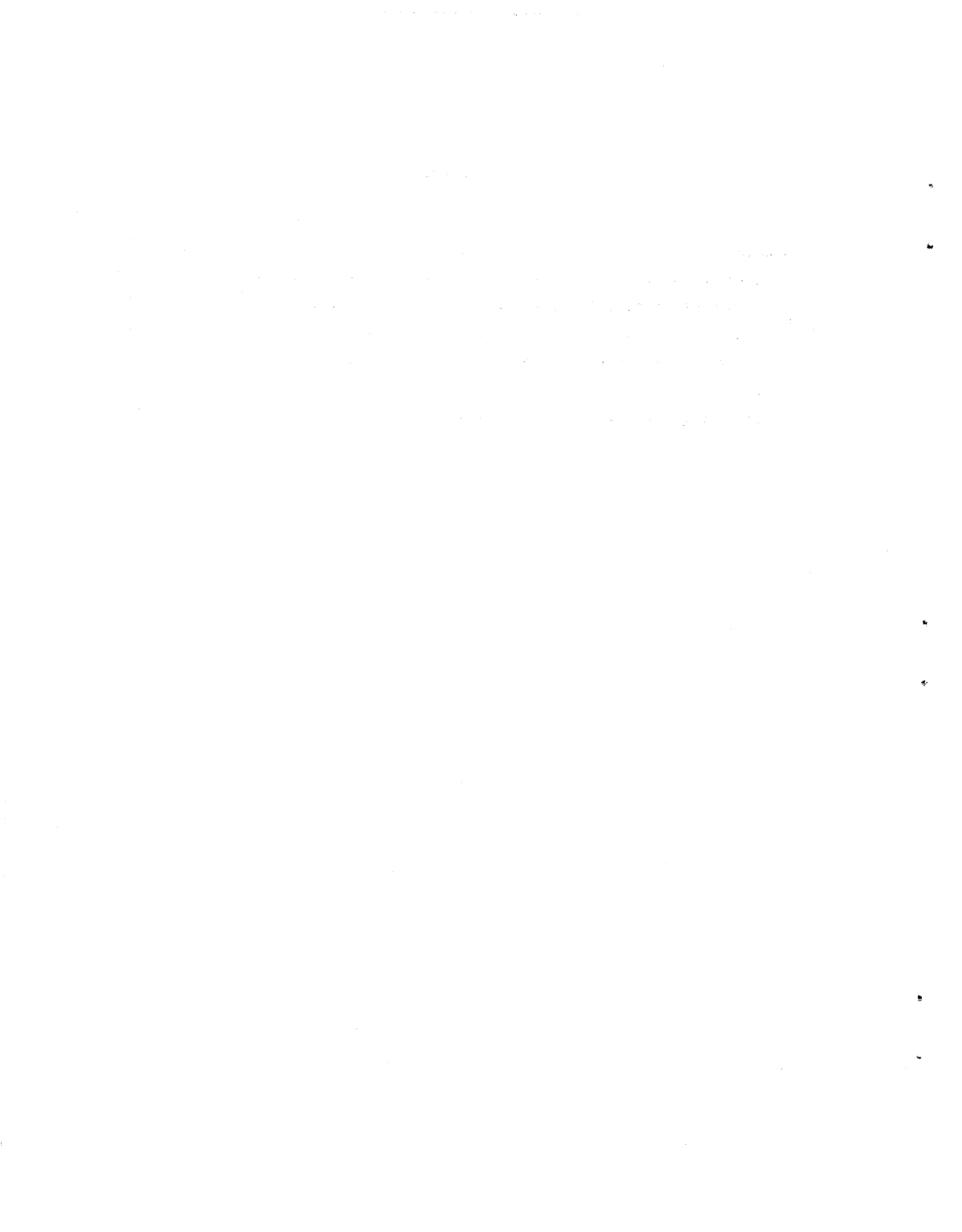
Submitted for publication in *Nuclear Technology*.

OAK RIDGE NATIONAL LABORATORY  
Oak Ridge, Tennessee 37830  
operated by  
UNION CARBIDE CORPORATION  
for the  
U.S. ATOMIC ENERGY COMMISSION



CONTENTS

Abstract . . . . .	1
Introduction . . . . .	1
Experiment Description . . . . .	5
Results . . . . .	9
Comparsion with Swelling Models . . . . .	15
Conclusions . . . . .	19
Acknowledgments . . . . .	20



## EFFECT OF HIGH HELIUM CONTENT ON STAINLESS STEEL SWELLING

F. W. Wiffen and E. E. Bloom

### ABSTRACT

Type 316 stainless steel specimens have been irradiated in the HFIR reactor at temperatures between 380 and 680°C to displacement damage levels up to 120 dpa and transmutation produced helium contents up to 6090 ppm. Swelling in solution annealed samples was found to be smaller than predicted by the helium swelling models but larger than predicted by fast reactor irradiation results, and the temperature dependence of swelling was also not in agreement with either prediction. Cold work reduced swelling for irradiation temperature up to 600°C but was ineffective at 680°C. For both annealed and cold worked materials the swelling was nearly temperature independent between 380 and 600°C but increased markedly at 680°C. Present models are inadequate to explain the swelling results in the presence of these high helium concentrations.

---

### INTRODUCTION

Two recent studies of controlled thermonuclear reactors (CTR) evolved design concepts that require a minimum extrapolation of technology outside of plasma containment.<sup>1,2</sup> In accord with this requirement, only those materials now commercially available were considered for reactor construction. The current state of development of refractory metal alloys appears to be inadequate for the intended application, so the selection narrows to iron or nickel base alloys as possible structural materials. The austenitic stainless steels appear most promising, and because of the considerable amount of development work that has gone into qualifying type 316 stainless steel for fast reactor applications, it has been chosen as the reference material in one design<sup>2</sup> and has also been considered in the other.<sup>1</sup>

---

<sup>1</sup>P. Bonanos and W. G. Price, Jr., Plasma Physics Laboratory, Princeton University, personal communication (June 1973).

<sup>2</sup>G. L. Kulcinski, R. G. Brown, R. G. Lott, and P. A. Sanger "Materials Radiation Damage Limitations in the Wisconsin Fusion Reactor Design," presented at ANS Winter Meeting, San Francisco, CA, Nov. 11, 1973, and to be published in *Nuclear Technology*.

Brager and Straalsund<sup>3</sup> have recently summarized the extensive body of data on the effect of fast reactor neutron irradiation on the microstructure of type 316 stainless steel. Although high levels of displacement damage have been achieved in fission reactors, these irradiations have not simulated the rate of transmutation reactions that would be achieved in CTR reactors. These results cannot be extrapolated directly to prediction of behavior in a CTR environment. Spectral differences account for the dissimilar transmutation rates; many reactions have thresholds that lie above the range of neutron energies found in fission reactors and others become more important with increasing neutron energy. The spectra in two positions of the EBR-II reactor and the spectrum in the first wall of a conceptual CTR, shown in Fig. 1, emphasize the lack of a high energy component of the neutron flux in the EBR-II reactor.

Calculated damage production rates in type 316 stainless steel in two CTR designs and in the EBR-II reactor are given in Table I. Note that the ratio of the helium production rate (in ppm/yr) to the displacement rate [displacements per atom (dpa) per year] is approximately 15 in the two CTR designs and only about 0.2 in EBR-II. Since there is ample proof that the presence of inert gases in metals may effect the

<sup>3</sup>H. R. Brager and J. L. Straalsund, *J. Nucl. Mater.* 46: 134 (1973).

Table I. Damage Rates in Type 316 Stainless Steel

Reactor	Neutronic Wall Loading MW/m <sup>2</sup>	Reactions per Year		
		dpa	He, ppm	H, ppm
CTR, Princeton <sup>a</sup>	1.87	30	460	
CTR, Wisconsin <sup>b</sup>	1.25	18	285	490
EBR-II		60 <sup>c</sup>	12 <sup>d</sup>	
HFIR		60 <sup>c</sup>	1900 <sup>d</sup>	~50

<sup>a</sup>P. Bonanos and W. G. Price, Jr., Plasma Physics Laboratory, Princeton University, personal communication (June 1973).

<sup>b</sup>G. L. Kulcinski, R. G. Brown, R. G. Lott, and P. A. Sanger, "Materials Radiation Damage Limitations in the Wisconsin Fusion Reactor Design," presented at ANS Winter Meeting, San Francisco, CA, Nov. 11, 1973, and to be published in *Nuclear Technology*.

<sup>c</sup>Calculated by Lindhard method, for displacement energy of 25 eV: H. T. Kerr and R. Q. Wright, Oak Ridge National Laboratory, personal communication (May 17, 1973).

<sup>d</sup>Taken from measured values.

damage state, the data from EBR-II irradiations, the source of the Brager-Straalsund correlations, cannot be used with confidence to predict the behavior in a CTR. Furthermore there is no model or theory available to explain the effect of helium on the irradiation response.

Helium in metals can act independently to degrade the properties of a reactor structural component. In combination with displacement damage, the synergistic effects on properties can only be determined experimentally. The static model developed by Barnes<sup>4</sup> gives an indication of the amount of swelling that can be expected if the helium were acting alone, but the model cannot be applied to CTR conditions without additional microstructural information. The effect of helium on ductility has recently been surveyed,<sup>5</sup> and concentrations near 30 ppm can reduce the tensile ductility of austenitic stainless steels to as little as one-third of the value for helium free material. The effect of helium levels greater than produced neutronically on the void swelling in EBR-II irradiation of stainless steel has been examined by Bloom and Stiegler.<sup>6</sup> They found that for irradiation at 390°C to  $7.4 \times 10^{21}$  neutrons/cm<sup>2</sup> the presence of 20 ppm He injected prior to irradiation enhanced the void concentration by more than a factor of 2. There are no results at higher neutron fluences that could establish the effect of helium on irradiation produced swelling. The combined effect of helium and displacement damage on ductility has been examined by Bloom,<sup>7</sup> showing that the effect is a greater reduction in ductility than can be accounted for on the basis of helium embrittlement alone. Although all of the work cited above is useful in defining the magnitude of the helium effects problem, in none does the helium level approach that expected for long term CTR service.

The Oak Ridge National Laboratory High Flux Isotope Reactor (HFIR) offers a unique ability to simulate more accurately the expected CTR radiation damage in alloys containing nickel by simultaneous production of displacement damage and transmutation helium. The observation of high helium content in nickel bearing alloys irradiated in thermal reactors led to the discovery of a two-step transmutation sequence that leads from a nickel isotope, through two thermal neutron captures, to the production of helium at relative rapid rates. The reactions and the reaction cross sections<sup>8</sup> are given in Eqs. (1) and (2),

---

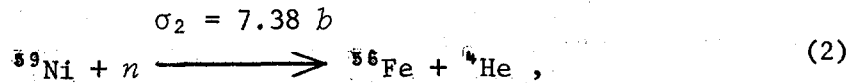
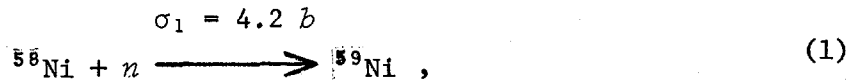
<sup>4</sup>R. S. Barnes, *J. Nucl. Mater.* 11: 135 (1964).

<sup>5</sup>D. Kramer, K. R. Garr, A. G. Pard, and C. G. Rhodes, "A Survey of Helium Embrittlement of Various Alloy Types," p. 109 in *Irradiation Embrittlement and Creep in Fuel Cladding and Core Components*, BNES, London, 1973.

<sup>6</sup>E. E. Bloom and J. O. Stiegler, *J. Nucl. Mater.* 36: 331 (1970).

<sup>7</sup>E. E. Bloom, "Correlation of Structure and Ductility of Irradiated Austenitic Stainless Steels," p. 93 in *Irradiation Embrittlement and Creep in Fuel Cladding and Core Components*, BNES, London, 1973.

<sup>8</sup>A. A. Bauer and M. Kangilaski, "Helium Generation in Stainless Steel and Nickel," *J. Nucl. Mater.* 42: 91-95 (1972).



where the cross sections given are for thermal neutrons. HFIR, a high flux thermal reactor, offers the fast flux necessary for rapid displacement damage production (high dpa levels) and the high thermal flux necessary to produce large amounts of helium in short times. The neutron spectrum of HFIR is compared to EBR-II and conceptual CTR's in Fig. 1. It can be seen that the flux above 0.6 MeV is greater in HFIR than in EBR-II. The damage production rates for 316 stainless steel irradiated in HFIR are also given in Table I. Comparison of the various data in Table I shows that HFIR provides a reasonable test facility for current CTR design needs, with displacement rates accelerated by about a factor of 2 and helium production rates by about a factor of 4 relative to the Princeton conceptual reactor.<sup>1</sup>

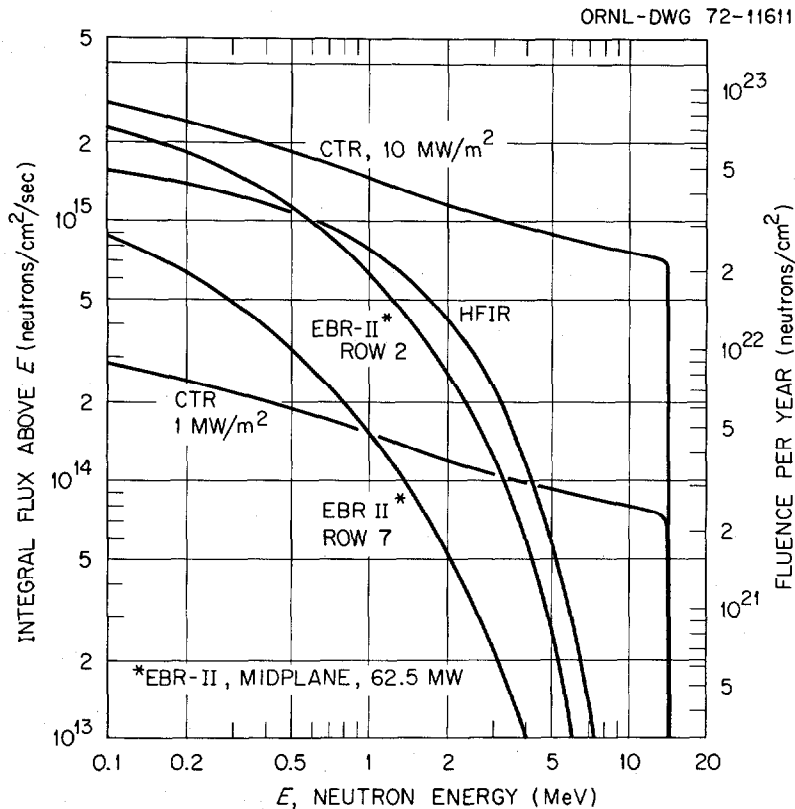


Fig. 1. Comparison of Integral Neutron Flux Spectrum for EBR-II, HFIR, and Conceptual CTR Reactor. Neutron fluence per year assumes a plant operating factor of 1.0.

Two problems remain with the attempt to use HFIR to simulate CTR radiation damage in type 316 stainless steel. First, the hydrogen production rate, approximately 50 ppm per year in HFIR, is well below the production rates calculated for a CTR. Second, the helium production rate is not constant in the HFIR reactor. Helium production is predicted<sup>8</sup> to be proportional to fluence to the second power, and has been demonstrated experimentally<sup>9</sup> to be more closely proportional to thermal fluence to the 1.68 power. This contrasts to the CTR where helium production will be linearly dependent on fluence. Even at the end of one year of HFIR irradiation the ratio of helium to dpa is approximately twice the value calculated for CTR design.

The high helium production rate in HFIR and the low rate in EBR-II, with nearly equal dpa rates in the two, thus effectively bracket the total radiation damage rates calculated for stainless steel in CTR's. Radiation effects in CTR service are expected to fall between the limits set by radiation effects found in the two fission reactors.

This paper reports the irradiation produced swelling of type 316 stainless steel, in both solution treated and cold worked conditions, for irradiation temperatures between 380 and 680°C. Neutron fluences ranged from 3.8 to  $8.7 \times 10^{22}$  n/cm<sup>2</sup> and helium contents at the end of irradiation ranged from 1790 to 6090 ppm. Subsequent papers will report mechanical properties; including tensile, creep and fracture properties; and microstructural effects in the same materials for similar irradiation conditions.

#### EXPERIMENT DESCRIPTION

The specimens used in this experiment were made of type 316 stainless steel prepared from material purchased from a commercial vendor. The composition is given in Table II, with all analyses within the specification limits for type 316 stainless steel. (These values represent the average of multiple analyses performed on this heat.) The final processing stages used to produce rod stock were: 0.5 in.-diam, hot-rolled rod was annealed 1 hr at 1200°C, cold swaged to 50% reduction in area. The rod was then solution annealed for 1 hr at 1050°C in Ar and rapidly cooled in the furnace cold zone. The rod was again swaged to reduce the area by 50% and samples were machined from part of the stock. These samples were annealed 1 hr at 1050°C (hereafter referred to as "solution treated" samples). Part of the remaining rod was annealed 1 hr at 1050°C and cold reduced another 20% by swaging, at which point "cold worked" samples were machined.

The HFIR is a thermal reactor which is uninstrumental in the flux trap region where these irradiations were performed. The thermal flux, integral flux above 0.1 MeV, and nuclear heating rates in stainless

---

<sup>9</sup>W. N. McElroy and H. Farrar IV, p. 187 in *Radiation-Induced Voids in Metals*, J. W. Corbett and L. C. Ianniello, Eds., AEC Symp. Ser. 26, CONF-710601 (April 1972).

Table II. Chemical Composition of Type 316 Stainless Steel<sup>a</sup>

Element	Cr	Ni	Mo	Mn	Si	Ti	C	P	S	N	B
wt%	18.0	13.0	2.58	1.9	0.8	0.05	0.05	0.013	0.016	0.05	0.0005

<sup>a</sup>Values given are averages of multiple determinations on this heat.

steel are given in Fig. 2 for the experimental position. The specimen geometry and experimental irradiation methods are shown schematically in Fig. 3. The specimen, 1.25 in. long, is made from 0.160 diameter rod and has cylindrical symmetry. The gage section is 0.75 in. long and 0.080 in. in diameter. Irradiation temperatures above water coolant temperatures ( $55^{\circ}\text{C}$ ) are attained by making use of the nuclear heating of the specimen itself. The heat generated in the specimen is balanced in design calculations against the thickness of the helium gas transfer gap to give the desired temperature gradient between the specimen and the specimen holder. Thin centering disks at the specimen ends minimize heat transfer through the specimen supports. Temperatures attained by this method were checked in a calibration experiment on SiC passive temperature monitors, using the geometry shown in the upper part of Fig. 3. The irradiation temperature determined from the post irradiation length change response on annealing, indicated agreement of  $\pm 25^{\circ}\text{C}$  with irradiation temperatures reported later in this paper. Heat transfer

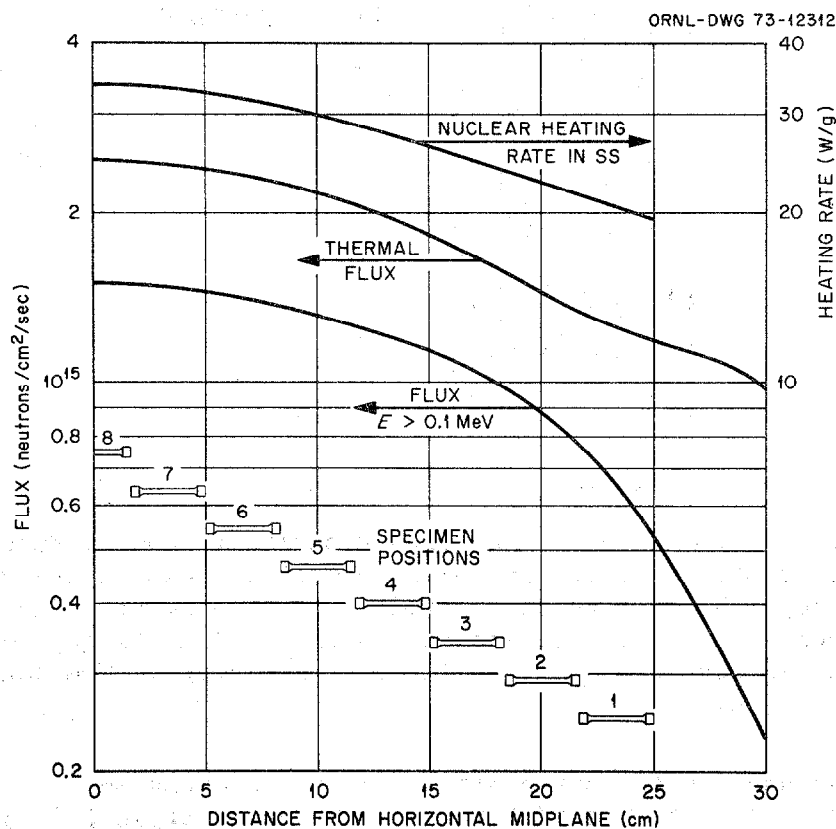


Fig. 2. Irradiation Parameters in the HFIR Reactor. The thermal flux, fast neutron ( $E > 0.1 \text{ MeV}$ ) and nuclear heating rates in stainless steel are given for the peripheral target position in the flux trap of the HFIR reactor. Specimen positions within the irradiation experiment are shown. The parameters given are for the reactor operating at full power, 100 MW.

ORNL-DWG 69-8936

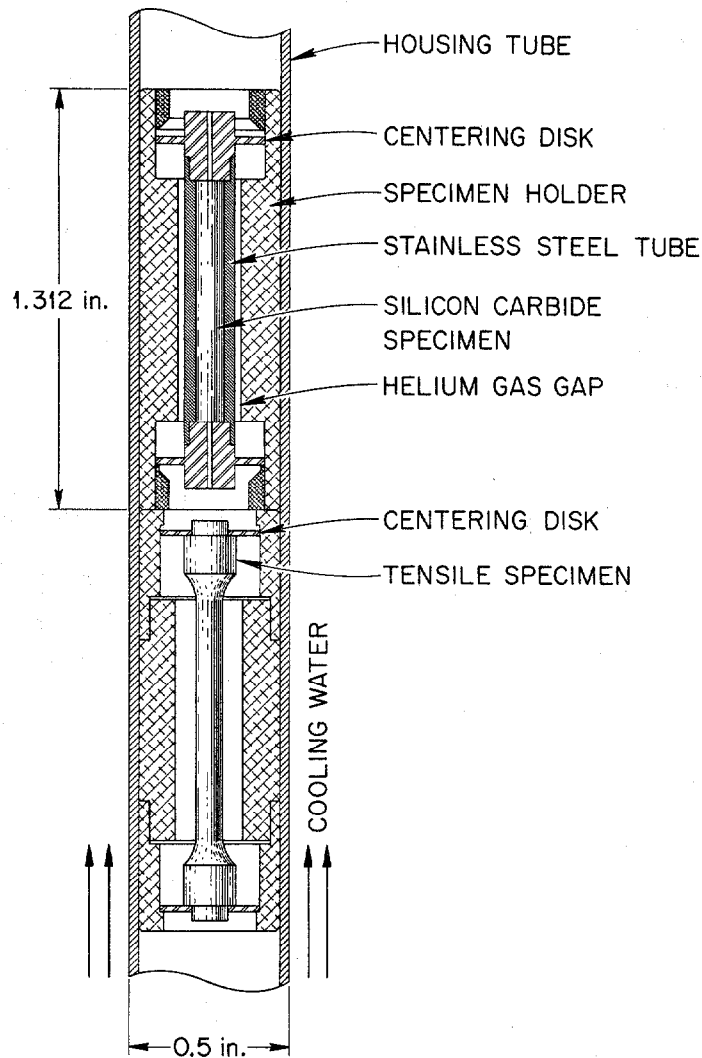


Fig. 3. Schematic of Irradiation Experiment Showing Method of Location of Tensile Specimen and Silicon Carbide Temperature Monitors in the Housing Tube of a Reactor Irradiation Experiment. The flow of heat generated in the specimen across the helium gas gap to the specimen holder controls the irradiation temperature. The method is discussed in text.

calculations show that temperature gradients in these small samples, for an irradiation temperature of  $570^{\circ}\text{C}$ , may be as great as  $70^{\circ}\text{C}$  along the gage section of the sample and  $160^{\circ}\text{C}$  from the sample center point to the outer "corner" of the buttonhead. Temperatures at the end of the specimen centering hub may be even lower than indicated by these gradients. Future microstructural evaluation at several locations on selected samples will be attempted to help define the temperature gradients in these samples.

Irradiation produced swelling was determined by measuring the immersion density of irradiated specimens and comparing to the density of control specimens. All samples were electropolished and density measurements were in water using photo flow as a wetting agent. The results reported are the average of five density determinations and were compared against internal standards in the density determination procedure. Swelling values determined by this method are accurate to  $\pm 0.1\%$  or better.

Transmission electron microscopy examination of these materials is made difficult by the very high radioactivity of the specimens. One tab cut for microscopy, approximately 0.015 in. thick and 0.080 in. in diameter, had activity greater than 10 R/hr at contact. This radiation is very penetrating and not easily shielded. A fully remote technique has been developed at ORNL for thinning and handling<sup>10</sup> these samples. For thinning stainless steel a solution of 6% HClO<sub>4</sub> in C<sub>2</sub>H<sub>5</sub>OH was used at an applied potential of approximately 38 V (current of 65 ma) operating at approximately 15°C.

## RESULTS

The swelling or specific volume increase produced by irradiation, equal to the density decrease measured by the immersion density technique, is given as a function of irradiation temperature and neutron fluence in Table III, for both solution annealed and cold worked samples. The specimen position relative to the reactor horizontal midplane is given in Fig. 2. The reported displacement levels (dpa) were calculated from the Lindhard method using a threshold energy of 25 eV and the fully detailed neutron spectrum of the reactor at the specimen position.<sup>11</sup> The helium content in atomic ppm was calculated from the empirical correlation developed by McElroy and Farrar,<sup>9</sup>

$$C = 9.8 \times 10^{-19} (\phi t)^{1.68} \text{ atoms He/g Ni} , \quad (3)$$

where  $\phi t$  is thermal neutron fluence. Comparison of the helium content calculated in this manner with one measured value from this set of specimens showed the calculated values to be higher than the experimental result. As a consequence all calculated helium contents were normalized to 0.65 of the calculated value. The helium values given in Table III are the normalized values. (The discrepancy in helium content will be further pursued when more measured values are available.)

<sup>10</sup>T. L. Chandler and C.K.H. DuBose, "Electron Microscopy Specimen Preparation in a Hot Cell," *Trans. Amer. Nucl. Soc.* 14: 881-82 (1971).

<sup>11</sup>H. T. Kerr and R. Q. Wright, Oak Ridge National Laboratory, personal communication (May 17, 1973).

Table III. Irradiation Conditions and Measured Swelling for Type 316 Stainless Steel Irradiated in the HFIR

Specimen Position <sup>a</sup>	Irradiation Temperature (°C)	Fluence >0.1 MeV (n/cm <sup>2</sup> )	Calculated Displacements <sup>b</sup> (dpa)	Calculated Helium Content <sup>c</sup> (ppm)	Measured Swelling, %	
					Solution Treated	20% Cold Worked
		×10 <sup>22</sup>				
4	379	7.05	97	4020	6.7	1.6
5	456	7.69	107	4820	8.7	0.80
6	528	8.27	114	5450	8.3	2.6
1	535	3.79	52	1930	3.5	0.52
8	574	4.21	58	1791 <sup>d</sup>	3.3	
7	602	8.71	119	5940	8.0	3.3
8	679	8.74	121	6090	14.1	16.8

<sup>a</sup>Specimen positions as shown in Fig. 2.

<sup>b</sup>The dpa calculated from Lindhard model. H. T. Kerr and R. Q. Wright, Oak Ridge National Laboratory, personal communication (May 17, 1973).

<sup>c</sup>Atomic concentration calculated by the formula  $C = 9.8 \times 10^{-19} (\phi t)^{1.68}$  atoms He/g Ni, where  $\phi t$  is thermal fluence. Formula from McElroy and Farrar in *Radiation-Induced Voids in Metals*, J. W. Corbett and L. C. Ianniello, Eds., AEC Symp. Ser. 26, CONF-710601 (April 1972), with normalization factor  $K = 0.65$  determined by measured value (d).

<sup>d</sup>Measured helium content.

The measured swelling in the solution treated samples ranged from 3.3 to 14.1% and showed little temperature dependence throughout the range of temperatures 380 to 600°C, with swelling values increasing with increasing helium content regardless of irradiation temperature. The data point at 679°C suggests that swelling may increase rapidly as temperature is increased above 600°C.

Swelling in the 20% cold worked samples ranged from 0.5 to 3.3% for irradiation temperatures of 600°C and lower, relatively insensitive to temperature, but did not vary in a consistent manner with helium or dpa level. Only at 679°C was the swelling comparable to that in the solution treated material, with slightly more swelling observed in the cold worked material. The results suggest that the cold worked structure recovered during irradiation at 679°C and thus lost its beneficial effect in suppressing the swelling.

The solution treated sample irradiated at 574°C has been examined by transmission electron microscopy. Figures 4 and 5 compare representative microstructures from this sample with microstructures of a sample irradiated at a similar temperature but to a lower fluence in the EBR-II reactor. The microstructural features of these two samples are summarized and compared in Table IV. The HFIR sample, with the higher helium content, contained an order of magnitude higher cavity concentration in the matrix, but the average cavity size was somewhat less than in the EBR-II sample. There is some association of cavities with precipitate particles in both samples, Fig. 4, but the degree of association is much greater in the sample irradiated in HFIR. In the latter sample each precipitate-matrix interface is lined with cavities. Another major difference between the two microstructures in Fig. 4 and 5 is the high concentration of cavities on the grain boundaries of the HFIR irradiated sample and the absence of boundary cavities in the fast reactor irradiated sample. Some of the grain boundary cavities in the HFIR sample appear to be elongated (Figs. 4 and 5). However, viewing these cavities stereographically shows that only the cavities which intersect one of the foil surfaces are elongated. Cavities that are contained entirely within the foil after thinning show an equiaxed appearance, with apparently no tendency for the cavity to elongate in the plane of the grain boundary.

It is generally believed that the cavities seen after EBR-II irradiation of stainless steel at 580°C are voids, with the pressure of contained gases well below the pressure necessary to stabilize equilibrium gas bubbles. In the HFIR-irradiated sample the grain boundary cavities and the cavities on precipitate-matrix interfaces are not void-like in character but are suggestive of equilibrium gas bubbles. In the matrix of this sample, well removed from grain boundaries and precipitates, the cavity concentration is  $1 \times 10^{14} \text{ cm}^{-3}$  with average diameter 525Å. The measured helium content of 1790 ppm sets an average gas content of  $1.54 \times 10^6$  atoms per cavity, assuming uniform distribution of the gas. The gas distribution in the case where all gas is contained in bubbles in equilibrium with surface energy,  $\gamma$ , is given<sup>4</sup> in terms of bubble diameter,  $\bar{d}$ , gas content,  $m$ , and bubble concentration,  $N$ , as:

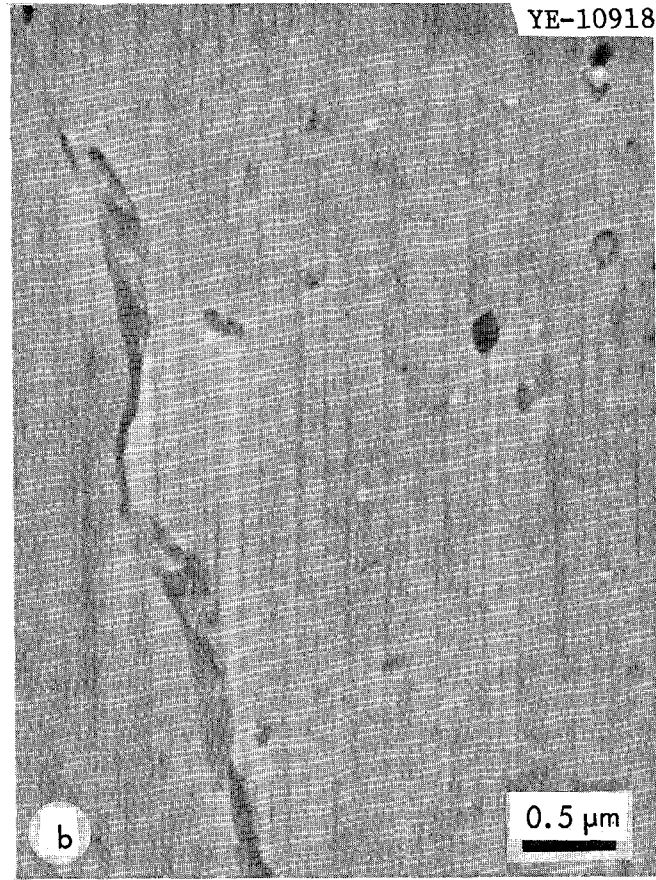
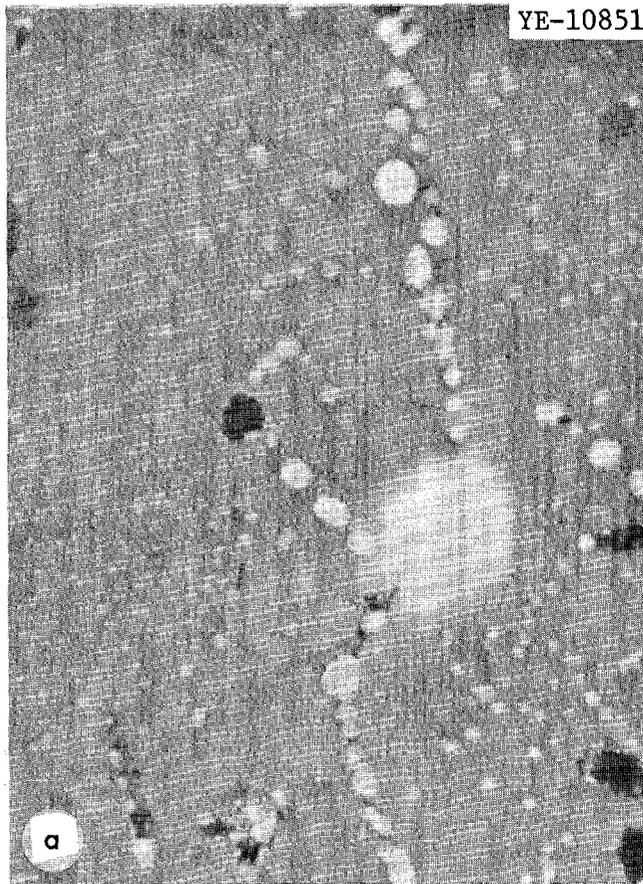


Fig. 4. Comparison of Microstructures in Solution Annealed Type 316 Stainless Steel. (a) Irradiated in HFIR at 575°C to  $4.2 \times 10^{22}$  n/cm<sup>2</sup> (58 dpa and 1790 ppm He). (b) Irradiated in EBR-II at 580°C to  $1.9 \times 10^{22}$  n/cm<sup>2</sup> (26 dpa and ~5 ppm He).

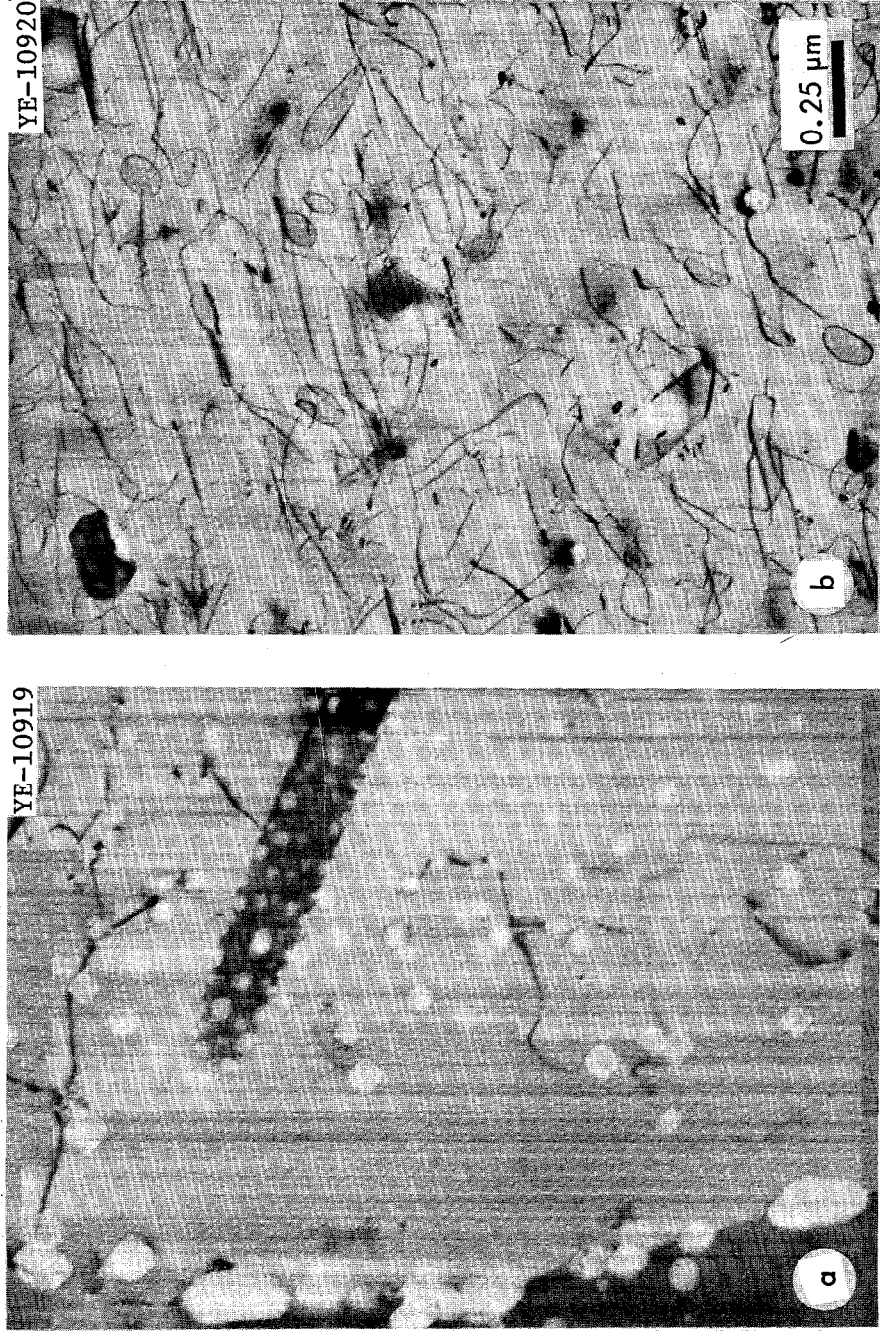


Fig. 5. Dislocation Structures in Solution Annealed Type 316 Stainless Steel Irradiated (a) in HFIR and (b) in EBR-II. Irradiation conditions as in Fig. 4.

Table IV. Comparison of Microstructures in Solution Annealed Type 316 Stainless Steel Irradiated in a Thermal Reactor (HFIR) and a Fast Reactor (EBR-II)

Parameter	Units	HFIR Irradiated	EBR-II Irradiated
Irradiation Temperature	°C	574	580
Fluence (>0.1 MeV)	$10^{22}$ n/cm <sup>2</sup>	4.2	1.9
Displacements	dpa	58	26
Transmutation Helium	ppm	1790	5 <sup>a</sup>
Cavity Concentration	$10^{13}$ cm <sup>-3</sup>	10.3	1.0
Average Cavity Diameter	Å	525 <sup>b</sup>	666
Calculated Cavity Volume	%	1.0 <sup>b</sup>	0.21
Measured Density Decrease	%	3.3	
Dislocation Line Concentration	$10^9$ cm <sup>-2</sup>	1.1	4
Dislocation Loop Concentration	$10^{12}$ cm <sup>-3</sup>	0	4.8
Dislocation Description		Line segments from large scale network, pinned on voids and precipitates. No complete loops.	Connected network, some large unfaulted loops, and faulted loops with average diameter 1700 Å.
Precipitates		One type of large, blocky precipitate, with average long dimension near 1μ.	Blocky M <sub>23</sub> C <sub>6</sub> and needle-like, smaller precipitate of unidentified type.

<sup>a</sup>Estimated value.

<sup>b</sup>Approximate values, based on relatively few measurements.

$$d^2 = \frac{3mkT}{2\pi\gamma N}, \quad (4)$$

where

$k$  = gas constant,  
 $T$  = absolute temperature.

Using this equation and the observed cavity size distribution, equilibrium is satisfied for a surface energy of  $\gamma = 2800$  ergs/cm<sup>2</sup>, approximately twice the value commonly taken for austenitic stainless steels in the temperature range of interest. However, no allowance was made for the gas content at grain boundaries and precipitate interfaces. While we expect to refine this comparison when more detailed microscopy has been completed, these calculations suggest that the cavities in this sample are near-equilibrium gas bubbles.

The dislocation microstructure of the HFIR and EBR-II irradiated samples are shown in Fig. 5, and dislocation line and dislocation loop densities are given in Table IV. The HFIR-irradiated sample contains only one quarter of the dislocation content of the EBR-II irradiated sample, with the dislocations in both samples present as highly interconnected networks. The EBR-II irradiated sample also contained some large, perfect loops and numerous faulted loops. There were no loops of either kind in the HFIR irradiated sample. There are also differences in the type and morphology of the precipitate particles produced by the two irradiations. The HFIR irradiated sample contained only one type of large, blocky precipitate, with average long dimension near  $1\mu$ . These have not yet been analyzed. In contrast, the EBR-II sample shows two types of precipitate, a blocky  $M_{23}C_6$  and a much smaller needle-like precipitate that has not been identified.

#### COMPARISON WITH SWELLING MODELS

In comparing these results to the predictions of various swelling models, the main features that have to be considered can be summarized as follows:

1. The swelling observed is greater than values reported for irradiation to similar fluences in EBR-II, with the values of 14 to 17% believed to be the greatest found in reactor irradiated stainless steels.
2. The swelling shows a very weak temperature dependence for irradiation temperatures up to 600°C. Swelling appears to increase rapidly between 600 and 680°C.
3. Cold work is effective in suppressing swelling up to 600°C in the presence of high helium concentrations, but is ineffective at 680°C, probably due to recovery of the cold worked microstructures.
4. The tendency of cavities to form on grain boundaries and precipitate interfaces and the approximate balance of calculated gas pressure and surface energy in cavities suggest that in the sample examined after 574°C irradiation the cavities are helium bubbles.

Although there are no available models which simultaneously treat swelling due to both high displacement damage (dpa) and high helium content, these processes have been treated individually. The swelling predicted by these models has been calculated and is compared to the measured swelling of solution treated samples in Table V.

The swelling due to displacement damage alone has been described empirically by Brager and Straalsund,<sup>12</sup> who developed equations to correlate the available data for swelling in EBR-II irradiations as a function of fluence and irradiation temperature. These equations have been used with the temperature and fluence corresponding to the present HFIR irradiations to calculate the swelling that would have been expected under fast reactor irradiation. The results are given in Table V. For purposes of comparison swelling was also calculated as a function of irradiation temperature at a constant fluence of  $8.0 \times 10^{22}$  n/cm<sup>2</sup> using the same equation. At this fluence the Brager-Straalsund equation predicts a swelling maximum of 8.2% at 497°C. At 380°C the predicted swelling is down to 0.82%, and at 680°C it is only 1.3%. Comparison of this predicted swelling due to the displacement damage alone with the observed swelling in the HFIR irradiation shows that in every case the fast reactor swelling equations predict less swelling than observed for the HFIR specimens. At 528°C, near the temperature for peak swelling in the fast reactor case, predicted swelling is very close to the measured swelling value. This suggests that swelling may be insensitive to helium content for cases where "void" swelling produces sufficient cavity volume to accommodate the gas. At both lower and higher temperatures the predicted swelling drops off rapidly with temperature away from the maximum, in sharp contrast to the measured swelling which shows only a small dependence on irradiation temperature. At 574°C, near the predicted peak swelling temperature and where the microstructural comparison is available, the observed cavity concentration and size are in good agreement with the predicted values from the Brager-Straalsund equations. Since the swelling agreement becomes worse at temperatures higher or lower than the maximum swelling temperatures, the cavity concentration and/or size, must be greater than predicted from these empirical equations.

The agreement in cavity concentration between the sample irradiated at 574°C and the prediction of the Brager-Straalsund equations is coincidental. The equations are based mainly on the behavior of one heat of type 316 stainless steel, and there is significant variation in void concentrations between different heats of this alloy.

In EBR-II irradiation the ORNL heat of type 316 stainless steel consistently shows much lower cavity concentrations than predicted by the equations. The result in the HFIR irradiation at 574°C shows an increased cavity nucleation rate, relative to EBR-II irradiation, due to the higher helium concentration. This is the same effect as reported by Bloom and Stiegler<sup>13</sup> using preinjected helium in EBR-II irradiated samples at much lower temperatures and fluences.

---

<sup>12</sup>H. R. Brager and J. L. Straalsund, *J. Nucl. Mater.* 46: 134 (1973).

<sup>13</sup>E. E. Bloom and J. O. Stiegler, *J. Nucl. Mater.* 36: 331 (1970).

Table V. Swelling in Solution Treated Type 316 Stainless Steel, Measured, Normalized, and Predicted by Models

Irradiation Temperature (°C)	Calculated Helium Content (ppm)	Swelling, %		
		Fast Reactor Model <sup>a</sup>	Due to He Alone <sup>b</sup>	Measured
379	4020	0.71	11	6.7
456	4820	5.27	16	8.7
528	5450	7.94	21	8.3
535	1930	1.17	5.8	3.5
574	1791	1.05	5.5	3.3
602	5940	4.50	28	8.0
679	6090	1.67	34	14.1

<sup>a</sup>Calculated from empirical formula for swelling of neutron-irradiated solution-treated type 316 stainless steel given by Brager and Straalsund, *J. Nucl. Mater.* 46: 134 (1973). Equations derived from irradiations that resulted in <30 ppm He.

<sup>b</sup>Approximate swelling for all helium in equilibrium bubbles, with constant bubble concentration of  $10^{14}/\text{cm}^3$ . Taken from Barnes, *J. Nucl. Mater.* 11: 135 (1964).

The second model that can be applied to the present experimental results is that due to Barnes<sup>14</sup> which assumes that the cavities are equilibrium bubbles and neglects any effect of displacement damage. In the Barnes model the swelling depends on the helium content, the concentration of bubbles, the temperature, and the specific surface energy, and can be obtained from Eq. (4). The model develops swelling values as a function of gas content of the sample using the Van der Waals equation of state for helium. Unfortunately, use of this model requires a knowledge of the cavity concentration for the different irradiation conditions, which is a structure and temperature sensitive parameter that cannot be calculated independently. Until cavity concentration data are available, the Barnes model cannot be fully evaluated, but it is useful to examine a limiting case. If we assume that the cavity concentration is a constant independent of irradiation temperature ( $1 \times 10^{14} \text{ cm}^{-3}$  as observed in one sample) and the surface energy is  $1000 \text{ ergs/cm}^2$  (as used by Barnes), the  $500^\circ\text{C}$  swelling values calculated by Barnes approximately fit the equation,

$$\frac{\Delta V}{V} = 2.4 \times 10^{-4} (C_{\text{He}})^{1.3}, \quad (5)$$

where  $\Delta V/V$  is the percent swelling and  $C_{\text{He}}$  is the helium content in atomic parts per million. The result was extended to the experimental irradiation temperatures using Barnes model in which the swelling for a fixed helium content and bubble concentration is proportional to the absolute temperature to the  $3/2$  power. Swelling values calculated in this way for the HFIR irradiated samples are shown in the column "Swelling Due to Helium Alone" in Table V. These values are from 1.6 to 3.5 times the experimentally observed swelling. The calculated swelling due to helium alone shows the same insensitivity to temperature as do the experimental results. Lack of agreement between calculated and measured swelling probably lies in the assumed values for cavity concentration and surface energy. It is possible to fit the swelling data by using some appropriate set of cavity concentration values. However, until cavity concentrations are determined by microscopy there is no valid basis for choosing these concentrations.

Proof that the assumption of a constant cavity density for all irradiated specimens is not adequate can be obtained from the data. The specimens irradiated at  $528$  and  $535^\circ\text{C}$  can be compared using a modified form of Eq. (5):

$$\frac{\Delta V}{V} = A(N, T)(C_{\text{He}})^{1.3}, \quad (6)$$

---

<sup>14</sup>R. S. Barnes, *J. Nucl. Mater.* 11: 135 (1964).

where  $A(N,T)$  is a function of cavity concentration,  $N$ , and temperature,  $T$ . The observed swelling of 3.5% for the sample irradiated at 535°C (1930 ppm He) thus predicts a swelling of 13.5% in the sample irradiated at 528°C (5450 ppm He). As the measured swelling in this sample was only 8.3%, it follows that  $A(N,T)$  was not constant and that the cavity concentration increased with increasing helium contents. Comparison of the swelling data at 602 and 679°C with swelling values given by Barnes shows that cavity concentrations of at least  $10^{15} \text{ cm}^{-3}$  will be required to give agreement between the predicted and observed swelling, an order of magnitude greater than the assumed constant cavity concentration of  $10^{14} \text{ cm}^{-3}$ .

### CONCLUSIONS

To evaluate the combined effects of displacement damage and helium production the HFIR reactor was used to irradiate type 316 stainless steel in the solution annealed and cold worked conditions at temperatures between 380 and 680°C. Displacement damage levels achieved in this irradiation ranged from 52 to 121 dpa, and the helium contents from 1791 to 6090 ppm. Swelling in the solution annealed samples ranged from 3.3 to 14.1%. Swelling was relatively temperature insensitive in the range 380 to 600°C, but significantly larger swelling occurred at the highest irradiation temperature, 679°C. Swelling in the cold worked samples was lower than in the solution treated samples, ranging from 0.5 to 3.3% in the temperature range 380 to 600°C. As in the solution annealed material, the greatest swelling was recorded at 680°C and the effectiveness of cold work in swelling suppression appears to break down about 600°C. In a sample irradiated at 574°C the microstructure was dominated by a very high concentration of small cavities believed to be helium bubbles. In contrast to the microstructure of samples irradiated in the EBR-II (where helium contents are low) the grain boundaries of the HFIR irradiated sample were heavily covered with cavities, and all precipitate interfaces and dislocations had cavities attached to them.

Comparison of the models which attempt to predict swelling in solution annealed type 316 stainless steel reveals that there is not a model which will completely explain swelling under the mixed irradiation conditions of high displacement damage production (high dpa) and high helium production. The comparisons suggest that the helium may dominate the swelling behavior. The empirical swelling equations developed from fast reactor irradiation programs<sup>12</sup> predict nearly the correct swelling in the middle of the temperature range investigated, that is near the peak in the fast reactor swelling equation. However, the temperature dependence predicted by the fast reactor equations is much different from that observed in this case. Swelling in the low helium, fast reactor irradiation drops off rapidly for temperatures above or below the temperature of maximum swelling whereas in the samples containing high helium the swelling is insensitive to temperature over the same temperature range.

The Barnes model<sup>14</sup> which treats swelling due to helium in equilibrium cavities in a solid comes closer to predicting the observed swelling.

behavior. Adjustment of the parameters in this model could probably bring swelling values into agreement, at least at some temperatures. However this model cannot be fully tested until microstructural information is available. In particular, the model is unable to predict the cavity concentration, which must be known for the model to be used to predict swelling. A truly adequate model to predict swelling must contain such an expression to predict the cavity concentration as a function of the irradiation parameters, including helium concentration. The relative insensitivity to temperature in the swelling produced by a high helium concentration in the Barnes model is close to the observed experimental behavior. Cold work is effective in suppressing swelling below temperatures of about 600°C. Comparison of this observation with the Barnes model for swelling due to helium suggests that in the cold worked sample the helium cavity density must be much higher than in the solution annealed material. This increased cavity density will accommodate the same amount of helium with a lesser degree of swelling, consistent with the observed swelling suppression.

Comparison of the swelling at similar temperatures and two helium levels showed that cavity concentration is increasing with neutron fluence (and increased helium content). Since swelling is reduced by increasing the cavity concentration, the greatest potential for control of the swelling lies in the development of alloy systems with high concentrations of nucleation sites, to nucleate the highest possible cavity concentration.

The tendency for helium bubbles to form on grain boundaries may lead to intergranular failure in stressed components well before swelling values as large as observed in this work can be realized. The increased swelling rate at the highest temperature, especially the breakdown of the swelling resistance of cold worked material at 680°C, suggests that stainless steel to be used in a CTR should operate only at temperatures of 600°C and lower.

The present work has not answered the effect of stress on the swelling. Recent theoretical work predicts<sup>15</sup> that the effect of stress on swelling will be moderate at 600°C but very large at 700°C and higher. When experimental verification of this higher temperature stress effect becomes available, it may add a further restriction to high temperature service.

#### ACKNOWLEDGMENTS

The authors would like to thank the many people at ORNL who contributed to the success of this work. A. F. Zulliger and J. W. Woods for design and construction of the experiments, C.K.H. DuBose for development of the thinning techniques and thinning the high activity stainless steel sample, J. O. Stiegler for constant interaction throughout the course of the work, the hot cell operations personnel for their skill and care in handling the samples, and to Stephanie Davision for preparation of the final manuscript copy.

---

<sup>15</sup>A. D. Brailsford and R. Bullough, *J. Nucl. Mater.* 48: 87 (1973).

## INTERNAL DISTRIBUTION

(3)	Central Research Library	J. M. Leitnaker
	ORNL - Y-12 Technical Library	W. R. Martin
	Document Reference Section	C. J. McHargue
(10)	Laboratory Record Department	P. Patriarca
	Laboratory Records, ORNL R.C.	H. Postma
	ORNL Patent Office	M. W. Rosenthal
	G. M. Adamson	Jacob Scheten
	R. G. Alsmiller	J. L. Scott
	D. S. Billington	D. Steiner
(10)	E. E. Bloom	J. O. Stiegler
	J. F. Clarke	D. B. Trauger
	F. L. Culler	H. A. Ullmaier
	J. E. Cunningham	T. N. Washburn
	J. H. DeVan	J. R. Weir, Jr.
	K. Farrell	(10) F. W. Wiffen
	A. P. Fraas	J. W. Woods
(3)	M. R. Hill	M. H. Yoo
	R. T. King	F. W. Young, Jr.
		A. Zucker

## EXTERNAL DISTRIBUTION

AMES LABORATORY, Iowa State University, Ames, IA 50010

M. S. Wechsler

ARGONNE NATIONAL LABORATORY, 9700 South Cass Avenue, Argonne, IL 60439

N. D. Dudey

B.R.T. Frost

M. Kaminsky

P. J. Persiani

M. Petrick

ATOMIC ENERGY RESEARCH ESTABLISHMENT, Culham, Abingden, Berkshire, UK

R. Carruthers

R. Hancox

G. M. McCracken

J.T.D. Mitchell

ATOMICS INTERNATIONAL, P.O. Box 309, Canoga Park, CA 91304

D. Kramer

H. Pearlman

BATTELLE-NORTHWEST, Pacific Northwest Laboratory, P.O. Box 999, Richland,  
WA 99352

J. L. Brimhall  
W. C. Wolkenhauer

BROOKHAVEN NATIONAL LABORATORY, 29 Cornell Avenue, Upton, Long Island,  
NY 11973

D. Gurinsky  
J. Powell

GENERAL ATOMIC INC., P.O. Box 81608, San Diego, CA 92138

G. R. Hopkins

GENERAL ELECTRIC CO., 310 Deguigne Drive, Sunnyvale, CA 94086

W. K. Appleby  
K. D. Challenger

HANFORD ENGINEERING DEVELOPMENT LABORATORY, P.O. Box 1970, Richland,  
WA 99352

T. T. Claudson  
J. Holmes  
J. Straalsund

INSTITUT FÜR FESTKÖRPERFORSCHUNG DER KERNFORSCHUNGSANLAGE, GmbH, 517 Jülich,  
West Germany

H. Conrads  
S. Foerster  
W. Schilling  
W. Schmatz

INSTITUT FÜR PLASMAPHYSIK, 8046 Garching, Munchen, Germany

R. Behrisch

JERSEY NUCLEAR COMPANY, 777-106th Avenue, N.E., Bellevue, WA 98004

H. K. Forsen

LAWRENCE LIVERMORE LABORATORY, University of California, P.O. Box 808,  
Livermore, CA 94550

R. Borg  
C. M. Logan  
W. B. Myers  
R. Werner

LOS ALAMOS SCIENTIFIC LABORATORY, P.O. Box 1663, Los Alamos, NM 87544

D. J. Dudziak  
W. V. Green  
F. L. Ribe  
J. Williams

MASSACHUSETTS INSTITUTE OF TECHNOLOGY, 77 Massachusetts Avenue, Cambridge,  
MA 02139

A. L. Bement, Jr.  
D. Rose  
K. C. Russell

NAVAL RESEARCH LABORATORY, Reactor Materials Branch, Metallurgy Division,  
Code 6390, Washington, DC 20375

D. J. Michel  
L. E. Steele

PRINCETON PLASMA PHYSICS LABORATORY, Princeton University, P.O. Box 451,  
Princeton, NJ 08540

P. Bonanos  
R. G. Mills  
W. G. Price, Jr.  
F. Tenney

SANDIA CORPORATION, P.O. Box 969, Livermore, CA 94550

W. Bauer

UNIVERSITY OF CALIFORNIA, Dept. of Chemical and Nuclear Engineering,  
Santa Barbara, CA 93106

G. R. Odette

UNIVERSITY OF CINCINNATI, Dept. of Materials Science, Cincinnati, OH 45221

J. Moteff

UNIVERSITY OF WISCONSIN, Dept. of Nuclear Engineering, Madison, WI 53706

G. L. Kulcinski

USAEC, DIVISION OF CONTROLLED THERMONUCLEAR RESEARCH, Washington, DC 20545

R. Bussard  
W. C. Gough  
R. L. Hirsch  
L. K. Price  
K. M. Zwilsky

USAEC, DIVISION OF PHYSICAL RESEARCH, Washington, DC 20545

L. C. Ianniello  
D. K. Stevens  
J. M. Teem

USAEC, DIVISION OF REACTOR RESEARCH AND DEVELOPMENT, Washington, DC 20545

G. W. Cunningham  
R. Klundt  
T. C. Reuther  
J. M. Simmons  
C. E. Weber

USAEC, OAK RIDGE OPERATIONS OFFICE, P.O. Box E. Oak Ridge, TN 37830

J. A. Lenhard  
Research and Technical Support Division

USAEC, SITE REPRESENTATIVES, OAK RIDGE NATIONAL LABORATORY, P.O. Box X,  
Oak Ridge, TN 37830

D. F. Cope  
C. L. Matthews

USAEC, TECHNICAL INFORMATION CENTER, P.O. Box 62, Oak Ridge, TN 37830

(2) Manager  
(17) For transmittal to ACRS